

175900-11-T

Annual Report

# ALL-OPTICAL BEAM CONTROL BY FORCED RAYLEIGH SCATTERING

## AD-A184 315

L.M. PETERSON  
Advanced Concepts Division  
DECEMBER 1986

DTIC  
ELECTE  
SEP 08 1987  
S D

Distribution Unlimited

DISTRIBUTION STATEMENT A  
Approved for public release;  
Distribution Unlimited

Defense Advanced Research Projects Agency  
1400 Wilson Blvd.  
Arlington, VA 22209



**ERIM** P.O. Box 8618  
Ann Arbor, MI 48107-8618

REPORT DOCUMENTATION PAGE

1a REPORT SECURITY CLASSIFICATION <b>UNCLASSIFIED</b>		1b. RESTRICTIVE MARKINGS	
2a SECURITY CLASSIFICATION AUTHORITY		3. DISTRIBUTION/AVAILABILITY OF REPORT  Unlimited	
2b DECLASSIFICATION/DOWNGRADING SCHEDULE			
4 PERFORMING ORGANIZATION REPORT NUMBER(S)  175900-11-T		5 MONITORING ORGANIZATION REPORT NUMBER(S) Air Force Office of Scientific Research	
6a NAME OF PERFORMING ORGANIZATION Environmental Research Institute of Michigan	6b. OFFICE SYMBOL (if applicable)	7a. NAME OF MONITORING ORGANIZATION Building 410 Attn: Dr. Lee Giles Bolling AFB, DC 20332	
6c ADDRESS (City, State, and ZIP Code) P.O. Box 8618 Ann Arbor, MI 48107		7b. ADDRESS (City, State, and ZIP Code)	
8a NAME OF FUNDING /SPONSORING ORGANIZATION Defense Advanced Research Projects Agency	8b OFFICE SYMBOL (if applicable)	9 PROCUREMENT INSTRUMENT IDENTIFICATION NUMBER	
8c ADDRESS (City, State, and ZIP Code) 1400 Wilson Blvd. Arlington, VA 22209		10 SOURCE OF FUNDING NUMBERS	
		PROGRAM ELEMENT NO	PROJECT NO
		TASK NO	WORK UNIT ACCESSION NO
11 TITLE (Include Security Classification)  All-Optical Beam Control by Forced Rayleigh Scattering			
12 PERSONAL AUTHOR(S) Lauren M. Peterson			
13a TYPE OF REPORT Annual	13b TIME COVERED FROM 2/15/85 TO 9/15/85	14 DATE OF REPORT (Year, Month, Day) December 1986	15 PAGE COUNT 57
16 SUPPLEMENTARY NOTATION ARPA Order 4952 Program Code 3D10		Contract Number F49620-84-0067 Contract Period: 6/15/84-6/15/87	
17 COSATI CODES		18 SUBJECT TERMS (Continue on reverse if necessary and identify by block number)	
FIELD	GROUP	Optical Computing Nonlinear Optics	
		Thermal Effects Optical Switching	
		Stimulated Scattering Forced Rayleigh Scattering	
19 ABSTRACT (Continue on reverse if necessary and identify by block number)  An analysis is presented to support the experimental efforts directed toward the achievement of all-optical beam control based upon nonlinear optical effects of thermal origin. Although stimulated thermal Rayleigh scattering (STRS) is the primary effect of interest, the analysis falls in the broader category of forced Rayleigh scattering (FRS) where the underlying principles are the same. The interference of two coherent beams of radiation is discussed quantitatively and serves as the driving mechanism for creating a thermally-induced phase grating in an absorbing liquid, which is also discussed quantitatively. The analysis shows that for our experimental conditions, an efficient thermal phase grating can be generated using laser pulses possessing a few microjoules of energy, and is being pursued experimentally using nanosecond laser pulses. A dye laser using a grazing incidence grating (Littman design) which was purchased for its narrower spectral linewidth and longer coherence length compared to our previous dye laser is also described.			
20 DISTRIBUTION/AVAILABILITY OF ABSTRACT <input checked="" type="checkbox"/> UNCLASSIFIED, UNLIMITED <input type="checkbox"/> SAME AS RPT <input type="checkbox"/> DTIC USERS		21 ABSTRACT SECURITY CLASSIFICATION <b>UNCLASSIFIED</b>	
22a NAME OF RESPONSIBLE INDIVIDUAL		22b TELEPHONE (Include Area Code)	22c OFFICE SYMBOL

ABSTRACT

An analysis is presented to support the experimental efforts directed toward the achievement of all-optical beam control based upon nonlinear optical effects of thermal origin. Although stimulated thermal Rayleigh scattering (STRS) is the primary effect of interest, the analysis falls in the broader category of forced Rayleigh scattering (FRS) where the underlying principles are the same. The interference of two coherent beams of radiation is discussed quantitatively and serves as the driving mechanism for creating a thermally-induced phase grating in an absorbing liquid, which is also discussed quantitatively. The analysis shows that for our experimental conditions, an efficient thermal phase grating can be generated using laser pulses possessing a few microjoules of energy, and is being pursued experimentally using nanosecond laser pulses.

A dye laser using a grazing incidence grating (Littman design) which was purchased for its narrower spectral linewidth and longer coherence length compared to our previous dye laser is also described.



Accession For	
NTIS CRA&I	<input checked="" type="checkbox"/>
DTIC TAB	<input type="checkbox"/>
Unannounced	<input type="checkbox"/>
Justification	
By	
Distribution /	
Availability Codes	
Dist	Avail and/or Special
A-1	

Left Blank Intentionally  
(page iv)

## PREFACE

The work reported here was performed in the Optical Sciences Laboratory, which is part of the Advanced Concepts Division at ERIM. The work was supported by the Defense Advanced Research Projects Agency under the direction of Dr. John A. Neff and was monitored by the Air Force Office of Scientific Research under Contract No. F49620-84-C-0067. Col. Robert Carter was program manager for the AFOSR during the initial phases of this program and was replaced by Dr. Lee Giles later on in the program.

This annual technical report covers work performed from 15 February 1985 to 15 September 1985. The principal investigator at ERIM was Dr. Lauren M. Peterson and Patrick Hamilton was a major contributor to the experimental work.

Left Blank Intentionally  
(page vi)

## CONTENTS

Abstract.....	iii
Preface.....	v
List of Figures.....	viii
List of Tables.....	ix
1. Introduction.....	1
2. Two-Beam Interference.....	3
3. Thermally Induced Refraction Index Change.....	7
4. Thermal Phase Grating.....	15
4.1 Forced Rayleigh Scattering (FRS).....	15
4.2 Stimulated Thermal Rayleigh Scattering (STRS).....	18
5. Spectral Purity Considerations.....	19
5.1 Stimulated Thermal Rayleigh Scattering (STRS).....	19
5.2 Forced Rayleigh Scattering (FRS).....	20
6. Nitrogen Laser Pumped Dye Laser.....	25
7. Summary and Conclusion.....	29
Appendix A. The Thermo-Optic Coefficient for Fluids.....	31
Appendix B. Refractive Index Effects Upon a Focused Gaussian Beam....	35
Appendix C. Optimizing the Absorption Coefficient.....	39
Appendix D. Thermal Diffusion.....	41
Appendix E. Reflection Hologram Diffraction Efficiency.....	45
Appendix F. Optical Switching Using Stimulated Rayleigh Scattering...	49
References.....	57

---

LIST OF FIGURES

Figure 2.1 Interference of Two Coherent Beams of Radiation Crossing at an Angle of  $2\theta$ .  $k_1$  and  $k_2$  are Radiation Wave Vectors and  $K$  is a Wave Vector for the Resulting Interference Pattern.....5

Figure 3.1 Focusing Geometry for a Gaussian Laser Beam.....8

Figure 4.1 Interference of Two Coherent Laser Beams and Probing by a Third Laser Beam.....17

Figure 6.1 LSI Grazing Incidence Dye Laser. GM - Grating Mount; DC - Dye Cell; RM - Rear Mirror; TM - Tuning Mirror Mount; TA - Tuning Arm; CL - Cylindrical Lens.....26

Figure B.1 Change of Focus in a Medium of Refractive Index  $n$ .....36

Figure E.1 Diffraction Efficiency for a Thick Reflective Phase<sup>4</sup> Hologram as a Function of Refractive Index Amplitude....47

LIST OF TABLES

Table I. Material Parameters for Selected Liquids [4].....12  
Table II. LSI Grazing Incidence Dye Laser Parameters Model 337130...27  
Table III. Characteristics for STRS and FRS.....43

Left Blank Intentionally  
(page x)

1  
INTRODUCTION

During the first six months of this program, efforts were directed toward Stimulated Thermal Rayleigh Scattering (STRS) based upon amplifier and generator experiments [1]. The observed gain was less than expected and could have been due to an insufficiently narrow laser linewidth or optical wash-out of the fringes in the phase grating produced in the STRS process. Several approaches which addressed this during the second six month period include: (1) the purchase of a narrow linewidth, long coherence length dye laser, (2) the change of the experimental geometry such that the thermally generated phase grating fringes were further apart making washout less likely, and (3) additional analysis and modeling to better understand the laser-medium interaction.

Section 2 provides the basic equations for interference of two beams of coherent radiation to produce spatial fringes. Section 3 derives the fundamental equations describing the change in refractive index,  $\Delta n$ , in an absorbing liquid due to the passage of optical radiation which is absorbed and thermalized. The  $\Delta n$  is assumed to be a result of the density change of the liquid which accompanies the rise in temperature due to the absorption of the laser energy. Section 4 effectively combines the analysis of the previous two sections and discusses the thermally induced phase grating which results from the interference of two beams of coherent optical radiation in the presence of a liquid to which an absorbing dye has been added. Used as an all-optical switch for a third or probe beam of radiation, this is described as forced Rayleigh scattering (FRS). Used as a switch or gain mechanism where one interfering beam is the pumping radiation and the second beam is spontaneously Rayleigh scattered

radiation, this may be referred to as stimulated thermal Rayleigh Scattering (STRS). Section 5 discusses the spectral purity of the laser which is required to assure that the spectral fringe pattern possesses high contrast and is adequately distributed in space. Section 6 describes the new Laser Science Inc. grazing-incidence-grating dye laser which was purchased to replace our Molelectron dye laser. The LSI laser provides a significant improvement in spectral purity and coherence length at approximately the same energy per pulse.

2  
TWO-BEAM INTERFERENCE

The intensity of electromagnetic radiation can be expressed as

$$I = \sqrt{\frac{\epsilon}{\mu_0}} \langle E_T^2 \rangle$$

$$= \epsilon_0 n c \langle E_T^2 \rangle$$

where  $\mu_0$  is the magnetic permeability of a non-magnetic medium,  $\epsilon$  and  $\epsilon_0$  are the dielectric permittivities of a material medium and vacuum respectively,  $n$  is the refraction index of the medium,  $c$  is the speed of light in a vacuum and  $E_T$  is the total field present; the pointed brackets denote a temporal average. For two interfering plane waves

$$\overline{E}_1 = \frac{1}{2} \overline{A}_1 e^{i(\omega_1 t - \overline{k}_1 \cdot \overline{r})} + \text{c.c.}$$

$$\overline{E}_2 = \frac{1}{2} \overline{A}_2 e^{i(\omega_2 t - \overline{k}_2 \cdot \overline{r})} + \text{c.c.}$$

we have

$$\overline{E}_T = \overline{E}_1 + \overline{E}_2 .$$

Assuming parallel polarizations of the two fields

$$E_T^2 = \frac{1}{4} A_1^2 e^{i(2\omega_1 t - 2\overline{k}_1 \cdot \overline{r})} + \frac{1}{2} A_1 A_2 e^{i[(\omega_1 + \omega_2)t + (\overline{k}_1 + \overline{k}_2) \cdot \overline{r}]}$$

$$+ \frac{1}{4} A_1^2 + \frac{1}{4} A_2^2 e^{i(2\omega_2 t - 2\overline{k}_2 \cdot \overline{r})}$$

$$+ \frac{1}{2} A_1 A_2^* e^{i \left[ (\omega_1 - \omega_2)t + (\bar{k}_1 - \bar{k}_2) \cdot r \right]} + \frac{1}{4} A_2^2 + \text{c.c.}$$

Performing the temporal averaging over many optical cycles we have for the intensity

$$I = \epsilon_0 c n \left\{ \frac{1}{4} A_1^2 + \frac{1}{2} A_1 A_2^* e^{i \left[ (\omega_1 - \omega_2)t + (\bar{k}_1 - \bar{k}_2) \cdot r \right]} + \frac{1}{4} A_2^2 \right. \\ \left. + \frac{1}{4} A_1^{*2} + \frac{1}{2} A_1^* A_2 e^{-i \left[ (\omega_1 - \omega_2)t + (\bar{k}_1 - \bar{k}_2) \cdot r \right]} + \frac{1}{4} A_2^2 \right\}$$

If  $A_1$  and  $A_2$  are real, then

$$I = \frac{1}{2} \epsilon_0 c n \left\{ A_1^2 + A_2^2 + 2 A_1 A_2 \cos \left[ (\omega_1 - \omega_2)t + (\bar{k}_1 - \bar{k}_2) \cdot r \right] \right\}$$

Since

$$I_m = \epsilon_0 c n \left\langle E_m^2 \right\rangle \\ = \frac{1}{2} \epsilon_0 c n A_m^2 \quad m = 1, 2$$

we can write

$$I = I_1 + I_2 + 2 \sqrt{I_1 I_2} \cos (\Delta \omega t + \bar{K} \cdot r) \quad (2.1)$$

where

$$\Delta \omega = \omega_1 - \omega_2$$

$$\bar{K} = \bar{k}_1 - \bar{k}_2$$

If  $\Delta \omega \ll \omega_1, \omega_2$  and  $2\theta$  is the angle between  $\bar{k}_1$  and  $\bar{k}_2$  as shown in Figure 2.1, then

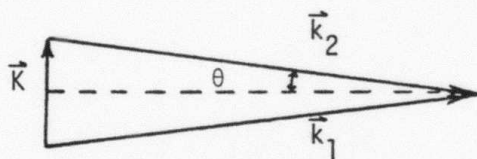
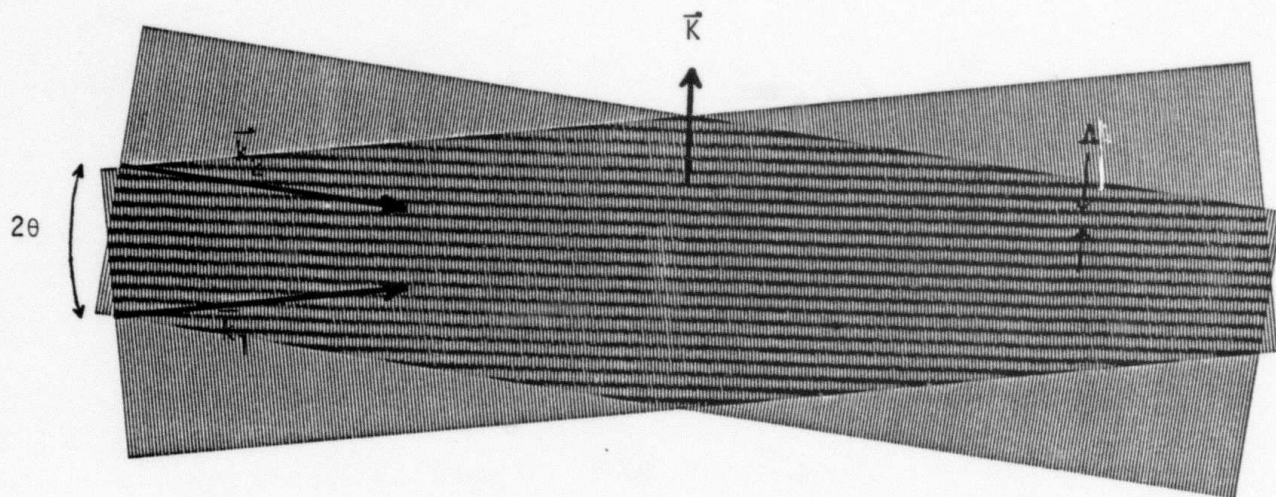


Figure 2.1 Interference of two coherent beams of radiation crossing at an angle of  $2\theta$ .  $\vec{k}_1$  and  $\vec{k}_2$  are radiation wave vectors and  $\vec{k}$  is a wave vector for the resulting interference pattern.

$$K = |\overline{K}| = 2k_1 \sin(\theta)$$

or

$$\Lambda = \frac{2\pi}{K} = \frac{\lambda}{2 \sin(\theta)}$$

For counter-propagating radiation,  $2\theta = 180$  degrees, and the spacing of the interference fringes,  $\Lambda$ , is  $\lambda/2$  or  $\lambda_0/2n$ . For small angles of interference,  $\Lambda$  can be much greater than  $\lambda$

$$\Lambda \doteq \frac{\lambda}{2\theta}$$

where  $\theta$  is the internal angle expressed in radians.

3  
THERMALLY INDUCED REFRACTION INDEX CHANGE

Laser radiation propagating through an absorbing medium leads to attenuation of the energy contained in the radiation beam. Thermalization of the absorbed energy subsequently leads to local rises in temperature and changes (usually decreases) in the refractive index of the medium. In the following, we quantify these effects in order to be able to predict the changes in refractive index which we might expect for our experimental conditions.

Radiation propagating through an absorbing medium is exponentially attenuated according to Beer's law

$$I(z) = I(0) e^{-\alpha z}$$

where  $I$  is the radiation intensity (watts/cm<sup>2</sup>),  $z$  is the propagation distance into the medium as shown in Figure 3.1, and  $\alpha$  is the (linear) absorption coefficient. We can write the intensity absorbed,  $\Delta I$ , in propagating a small distance  $\Delta z$  as

$$\Delta I = -\alpha I(z) \Delta z \quad (3.1)$$

Focusing of the radiation can be viewed as a converging cone of light which concentrates the light to a near-cylinder whose diameter,  $\delta$ , is twice the beam waist and whose length,  $l$ , is twice the confocal beam parameter or Rayleigh range [2]. We should remind ourselves that the intensity,  $I$ , is not uniform in this cylindrical focal volume but has a Gaussian profile in the transverse direction,  $r$ , if the laser beam is a spatially pure, single TEM<sub>00</sub> mode. That is

$$I(r, z) = I(0) e^{-2r^2/w(z)^2}$$

where the peak intensity is

$$I(0, z) = \frac{P(z)}{\pi w^2(z)} \quad \left( \frac{\text{watts}}{\text{m}^2} \right)$$

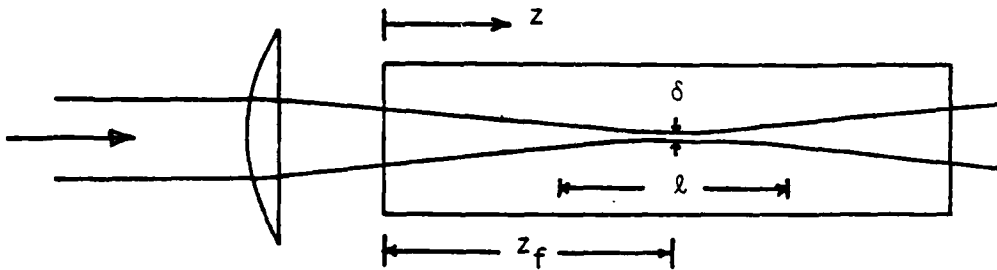


Figure 3.1 Focusing geometry for a Gaussian laser beam

$P$  is the total optical power\* in the beam at position  $z$  and  $w$  is the radius of the beam at position  $z$  as measured to the  $1/e^2$  intensity point.  $P$  is a function of  $z$  due to the absorbing nature of the propagation medium and  $w$  is a function of  $z$  due to the focusing (or divergence) of the beam. In the focal region, the peak intensity is a relatively constant

$$I(0, z_f) = \frac{P(0) e^{-\alpha z_f}}{\pi w_0^2} \quad (3.2)$$

where  $w_0 = w(z_f)$ .

If a pulsed laser is used, the instantaneous power changes with time. Since thermalization times are very fast ( $< 10^{-10}$  sec) for liquids [3], the power coupled into the medium as thermal energy closely follows the laser pulse temporal profile. If the pulse is much faster than the thermal diffusion time of the medium, energy is cumulatively deposited to create a monotonically rising temperature in the medium. The final temperature therefore depends upon the energy deposited in the medium per pulse. Assuming fluorescence to represent an insignificant loss of energy and assuming that all

---

\*For a Gaussian beam,

$$\begin{aligned} P &= \int I dA \\ P &= \int_0^{\infty} I(r) 2\pi r dr \\ &= I(0)\pi \int_0^{\infty} e^{-2r^2/w^2} 2r dr \\ &= I(0)\pi w^2 \end{aligned}$$

absorbed radiation energy is thermalized, we have for the energy deposited per unit volume per pulse at the center of the Gaussian beam profile

$$\Delta q(z) = \int_0^{\infty} \frac{\Delta P(z,t)}{\Delta V} dt = \int_0^{\infty} \frac{\Delta I(z,t)}{\Delta z} dt .$$

Using Eqs. (3.1) and (3.2), we have in the focal region

$$\begin{aligned} \Delta q(z_f) &= \int_0^{\infty} \alpha \frac{P(0,t) e^{-\alpha z_f}}{\pi w_0^2} dt \\ &= \int_0^{\infty} \alpha \frac{P_0(0,t) e^{-\alpha z_f}}{\pi w_0^2} dt \\ &= \alpha \frac{\mathcal{E}_0 e^{-\alpha z_f}}{\pi w_0^2} \left( \frac{\text{Joules}}{\text{m}^3} \right) \end{aligned}$$

where  $\mathcal{E}_0$  is the total energy of the laser pulse as it enters the absorbing medium.

The specific heat at constant pressure is defined as

$$c_p = \frac{1}{\rho V} \frac{\Delta Q}{\Delta T} \left( \frac{\text{Joule}}{\text{Kgm}^\circ\text{K}} \right)$$

where  $\rho$  is the medium density and  $\Delta Q$  is the energy required to raise the temperature of a volume  $V$  by an amount  $\Delta T$ . Solving for  $\Delta T$  and using  $\Delta Q = V \Delta q$ , we have for the rise in temperature of a medium due to absorption of optical radiation in the focal region

$$\Delta T = \frac{\alpha}{\rho c_p} \frac{\mathcal{E}_0 e^{-\alpha z_f}}{\pi w_0^2} .$$

This is the maximum  $\Delta T$  at the center of the Gaussian profile.  $\Delta T$  as a function of  $r$  is

$$\Delta T(r) = \frac{\alpha}{\rho c_p} \frac{\mathcal{E}_0}{\pi w_0^2} e^{-\alpha z_f} e^{-2r^2/w_0^2} \quad (3.3)$$

Although the absorbing medium may be optically dense, we have assumed that the radiation intensity does not change much throughout the focal region. If this is not a good assumption then the  $z_f$  should be changed to a variable  $z$ , and  $\Delta T$  becomes a function of  $z$  as well as  $r$ ,  $\Delta T$  being largest for small  $z$  within the focal volume. Outside of the focal volume,  $w$  becomes dependent upon  $z$  also and is always greater than  $w_0$ .

Thermally induced refractive index changes are primarily due to changes in density produced by the temperature change. The thermo-optic coefficient,  $dn/dT$ , discussed in Appendix A, can be modeled using the Lorentz-Lorentz relation for fluids. One obtains

$$\frac{dn}{dT} = - \frac{(n^2 - 1)(n^2 + 2)}{6n} \beta_V \quad (3.4)$$

where  $\beta_V$  is the thermal coefficient for volume expansion of the fluid. For liquids,  $\beta_V$  is on the order of  $10^{-3}$  as is the value of  $dn/dT$ . Table I presents parameters of interest for selected liquids. The change in index  $\Delta n$  is

$$\Delta n = \frac{dn}{dT} \Delta T \quad (3.5)$$

or, using Eq. (3.3)

$$\Delta n(r) = \frac{dn}{dT} \frac{\alpha}{\rho c_p} \frac{\mathcal{E}_0}{\pi w_0^2} e^{-\alpha z_f} e^{-2r^2/w_0^2}$$

and from Eq. (3.4), we have finally

$$\Delta n(r) = - \frac{(n^2 - 1)(n^2 + 2)\alpha}{6n \rho c_p} \frac{\mathcal{E}_0}{\pi w_0^2} e^{-\alpha z_f} e^{-2r^2/w_0^2} \quad (3.6)$$

Table I. Material parameters for selected liquids [4]

Liquid	n	$\rho$ (gm/cm <sup>3</sup> )	$C_p$ (erg/g $\cdot$ K)	$\beta_v$ ( $^{\circ}$ K <sup>-1</sup> )	$\lambda_T^a$ (mw cm <sup>-1</sup> K <sup>-1</sup> )	measured <sup>b</sup> calculated <sup>c</sup> dn/dT ( $^{\circ}$ K <sup>-1</sup> )	$t_{relax}^d$ (nsec)	$V_{sound}$ (cm/sec)	$\Gamma_B^e$ (MHz)	$\Gamma_R^f$ (MHz)
Carbon tetrachloride	1.46	1.591	$0.84 \times 10^7$	$1.18 \times 10^{-3}$	1.07	--	0.13	$0.95 \times 10^5$	630	18
Acetone	1.36	0.791	2.1	1.32	1.6	--	--	1.19	270	21
Methyl alcohol	1.33	0.794	2.5	1.18	2.0	--	0.013	1.21	300	12
Carbon disulfide	1.63	1.263	0.95	1.14	--	--	2.83	1.17	65	37
Benzene	1.50	0.880	1.7	1.18	--	$10.05$	--	1.17	350	27
Ethyl ether	1.35	0.715	2.3	1.51	1.32	$6 \times 10^{-4}$	--	1.03	290	16
Water	1.33	1.343	4.2	0.20	1.37	6	--	1.46	380	26
Ethyl alcohol	1.36	0.800	2.4	1.12	6.04	--	1.7	1.21	--	--
					1.7	4	4.58			

a) Thermal conductivity [6] p. 4-85.

b) AIP Handbook [6].

c) From equation (A.6) for  $\lambda=486$  nm;  $\beta_v$  from [6] p. 4-75.

d) Thermal relaxation time, from Hertzfeld and Litovitz [3].

e) Brillouin linewidth [5]; these values are 1.2 times greater than those presented by Shen [15], Table 11.1.

f) Rayleigh linewidth calculated from  $2\lambda_T k^2 / \rho C_p$ ;  $k=|k_L - k_S| = 2\pi/\lambda$ ;  $\lambda=694$  nm,  $180^{\circ}$  scattering.

This  $\Delta n$  represents the change in refractive index of a liquid medium from its equilibrium value due to the passage of a pulse of laser radiation which is absorbed by the liquid. We have assumed that the laser pulse is rapidly and efficiently thermalized and that the ensuing temperature change is responsible for the refractive index change. For a uniform Gaussian,  $TEM_{00}$  mode laser beam, the transverse profile of  $\Delta n$  is also Gaussian distributed.

In Appendix E it is shown that a  $\Delta n$  on the order of  $10^{-3}$  leads to good diffraction efficiency for a real-time thermally-induced phase grating. Using Eq. (3.5) and Table I, this corresponds to a  $\Delta T$  of only 1 or 2°K. Equation (3.6) and Table I allow the determination of the laser pulse energy  $\mathcal{E}_0$  corresponding to this value of  $\Delta n$ .  $\mathcal{E}_0$  is found to be on the order of a few microjoules for a beam focused to a waist radius of about 10  $\mu\text{m}$ . For a laser pulse of a few nanoseconds in duration, this corresponds to a kilowatt of peak power.

Left Blank Intentionally  
(page 14)

4  
THERMAL PHASE GRATING

In Section 3 we considered the thermal heating of a liquid due to the passage of laser radiation which is absorbed by that liquid. Since a single laser beam was considered, the temperature change and therefore the refractive index change was assumed to be uniform (or at least slowly varying) in the longitudinal direction and Gaussian distributed in the transverse direction. In Section 2 we considered the coherent interference of two beams of radiation which resulted in a beat pattern of the two beams. Equation (2.1) summarizes this interference. If the beams are copropagating but have different frequencies, a temporal beat note results. If the beams are the same frequency but propagate in different directions, stationary spatial fringes result. If the two beams are of different frequency ( $\Delta\nu$ ) and direction ( $\vec{k}_1 - \vec{k}_2 = \vec{K}$ ), a moving spatial fringe pattern results whose velocity is

$$v = \frac{\Delta\nu}{K} . \quad (4.1)$$

Combining the results of Sections 2 and 3, we can expect the interference of two beams of coherent radiation in an absorbing medium to produce a thermal grating which matches the spatial interference fringe pattern. Refractive index changes due to the temperature changes result in a phase grating. Motion of the interference pattern due to the mismatches in the frequencies (possibly due to limited temporal coherence), of the two interfering beams can lead to a washing out of the fringes since a thermal gradient persists for times on the order of the Rayleigh (diffusion) lifetime for the medium, as discussed in Appendix D.

#### 4.1 FORCED RAYLEIGH SCATTERING (FRS)

In forced Rayleigh scattering [7], two coherent beams of laser radiation are allowed to interfere, usually in an absorbing medium.

The angle between the two beams is usually small such that a fringe pattern or phase grating is produced whose spatial period is large compared to the radiation wavelength (i.e.,  $\theta$  small,  $\Lambda \gg \lambda$ ). A third laser beam, usually at a different wavelength, is used to probe the presence of the phase grating and to measure its decay thereby allowing the determination of thermal relaxation and diffusion properties of the medium. Although FRS has been primarily used as a measurement tool in thermal spectroscopy, it could also be used as an all-optical switching technique.

Figure 4.1 shows two spatially and temporally coherent pump beams at wavelength  $\lambda_g$  interfering at a small angle  $2\theta$  to generate a phase grating of spacing

$$\Lambda = \frac{\lambda_g}{2\theta} . \quad (4.2)$$

A probe beam at wavelength  $\lambda_r$  incident upon the phase grating at the Bragg angle  $\phi$  with respect to the fringe planes, where

$$\phi = \frac{\lambda_r}{\lambda_g} \theta , \quad (4.3)$$

is deflected (diffracted) by an angle  $2\phi$  as shown making an angle of  $-\phi$  with respect to the fringe planes. Although the figure is drawn for  $\lambda_r$  greater than  $\lambda_g$ , a  $\lambda_r$  less than  $\lambda_g$  is equally acceptable.  $\lambda_r = \lambda_g$  is also possible in which case  $\phi = \theta$ , although stray pump radiation may be a concern. This wavelength degenerate case is attractive from an alignment and cascading point of view but leads to a deflected beam which is counterpropagating along the same path as one of the pump beams. An appropriately placed beam splitter or the use of orthogonal polarizations should allow the separation of the deflected or switched probe beam from the pump beam.

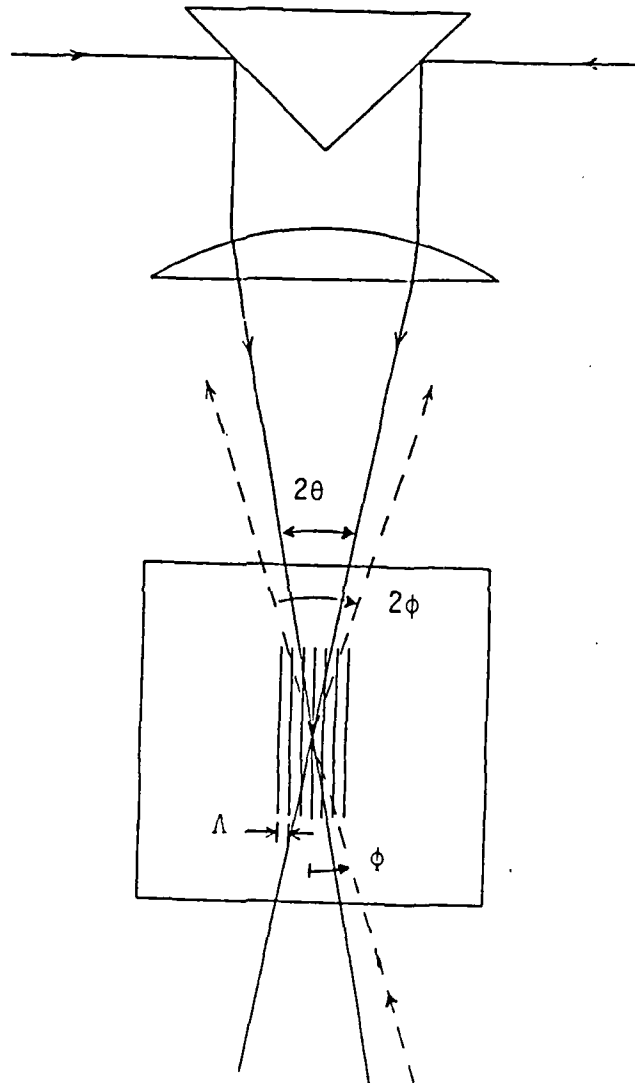


Figure 4.1 Interference of two coherent laser beams and probing by a third laser beam.

#### 4.2 STIMULATED THERMAL RAYLEIGH SCATTERING (STRS)

Stimulated thermal Rayleigh scattering is related to forced Rayleigh scattering in that they both rely upon a generated phase grating through absorption of pump radiation, thermalization of the absorbed energy, and refractive index changes due to the temperature change. In FRS, the phase grating is produced by the interference of two pump laser beams (derived from the same laser to assure coherence) at an angle of  $2\theta$  chosen by the experimenter, and subsequent diffraction of a third or probe beam of laser radiation by the phase grating. STRS may be viewed as a similar process where only a single pump beam is used. The phase grating results from the interference of pump radiation with spontaneous Rayleigh backscattering due to random thermal fluctuations (noise) in the material medium. One might consider STRS as a special degenerate (in angle and wavelength) case of FRS where the pump and probe are indiscernible as a single beam. Pump/probe radiation is backscattered, or diffracted by the phase grating through an angle  $2\theta$  equal to  $180^\circ$ . This backscattered radiation interferes with the incoming pump radiation to further amplify the phase grating which in turn amplifies the backscattering. The amplification or gain for STRS is exponential, and for sufficiently intense pump radiation, the backscattered STRS may correspond to an effective reflectivity approaching 100 percent. There is no gain associated with FRS and the reflectivity depends upon the magnitude of  $\Delta n$  for the phase grating and the interaction length of the phase grating.

5  
SPECTRAL PURITY CONSIDERATIONS

### 5.1 STIMULATED THERMAL RAYLEIGH SCATTERING (STRS)

Nonlinear optical interactions often require radiation with significant spectral purity or equivalently, an adequate coherence length. In backward STRS two counterpropagating radiation beams, a pump beam and a signal beam, beat together to generate a phase grating which Bragg reflects the pump radiation into the signal beam, thereby amplifying the latter. Equation (2.1) describes the beating process with  $K = 2k_1$ , or  $\Lambda = \lambda/2$ , for 180 degree STRS of two perfectly monochromatic waves. A realistic beam of laser radiation will have some small but finite spectral breadth associated with it, or it may have discrete spectral components such as longitudinal modes.

We wish to consider two counter-propagating beams each composed of two frequency components  $\omega_a$  and  $\omega_b$ . Beating of the two beams with their own counter-propagating components, leads to two separate standing waves of spatial periodicity  $\Lambda_a$  and  $\Lambda_b$ . (There is also a moving wave corresponding to the beat between  $\omega_a$  and  $\omega_b$  but this generally leads to washed out fringes.) Superposition of these two standing waves patterns of high spatial frequency,  $K_a$  and  $K_b$  leads to a resultant standing wave of low spectral frequency  $K'$  where

$$K' = K_b - K_a$$

or

$$\Lambda' = \frac{2\pi}{K_b - K_a}$$

If several frequency components (or even a continuum of frequencies) are present, the region of well-defined interference is of length  $\Lambda'$ , proportional to the reciprocal of the optical spectral bandwidth

$$\Lambda' = \frac{1}{\Delta\tilde{\nu}} = \frac{c}{\Delta\nu} = \frac{\lambda^2}{\Delta\lambda}$$

where  $\Delta\tilde{\nu}$  is expressed in wavenumber ( $\text{cm}^{-1}$ ),  $\Delta\nu$  is temporal frequency (Hz), and  $\Delta\lambda$  is wavelength spread ( $\mu\text{m}$ ). This is to say that the coherence length,  $\Lambda'$ , of the laser should be greater than or equal to the interaction region (i.e. the length of focus).

The length of the focal volume,  $l$ , for a Gaussian  $\text{TEM}_{00}$  laser beam is

$$l = 2 \frac{\delta^2}{\lambda} = 2F^2\lambda$$

where  $\delta$  is the focus diameter (to  $1/e^2$  intensity) and  $F$  is the f-effective f-number. For our Molelectron SP-10 dye laser we measured the coherence length to be less than 1 mm using a Michelson interferometer. For our LSI dye laser (Section 6) we measured it to be 3 mm.

## 5.2 FORCED RAYLEIGH SCATTERING (FRS)

In STRS, the phase grating is continually driven throughout the duration of the pulse. When the pulse has terminated, the effect is done. In FRS, two optical beams drive the phase grating. Although they usually originate from the same laser, there may be slightly different path lengths involved. A different path length can lead to a frequency difference between the interfering beams and therefore motion of the fringes in a direction perpendicular to the fringe planes. This motion can lead to washout of the phase grating with time. Also, since FRS utilizes a third or probe beam which may be a

long pulse, CW, or time delayed compared to the two pump beams, the persistence of the phase grating (possibly for microseconds) after the pump beams have terminated can be important.

Adequate temporal coherence is required between the two pump beams in order to produce a stationary or nearly stationary fringe pattern. If the frequencies of the two beams are not adequately matched, then the interference pattern will be moving in a direction perpendicular to the fringe planes. At best, a weak phase grating will result, and at worse, the grating will be totally washed out. If the fringe pattern moves slowly enough that the phase grating decays and is replenished at a slightly displaced position so as to follow the fringe pattern, then a strong phase grating can result. The persistence of the phase grating, or its decay time, is determined by thermal diffusion of energy from the high temperature (low density, high index) regions of the grating.

If  $t_v$  represents the time for a moving fringe (due to a frequency mismatch  $\Delta\nu$ ) to move one spatial period  $\Lambda$ , then from Eq. (4.1)

$$t_v = \frac{\Lambda}{v} = \frac{1}{\Delta\nu}$$

since  $K = 2\pi/\Lambda$ . Appendix D shows that  $t_d$ , the thermal decay or diffusion time, is

$$t_d = \frac{1}{DK^2} = \frac{1}{D} \left( \frac{\Lambda}{2\pi} \right)^2$$

or,

$$t_d = \frac{1}{D} \left( \frac{\lambda_g}{4\pi\theta} \right)^2$$

using Eq. (4.2). The diffusion time goes as the square of the grating period,  $\Lambda$ , or inversely as the square of interference angle, being greatest for small angles and a minimum for backscattering

where  $\theta$  must be replaced by  $\sin \theta = 1$ . If  $\Delta\nu$  is small enough such that  $t_v$  is much larger than both  $t_d$  and the pump pulse duration, then the thermally generated phase grating is stationary and persists for a time  $t_d$  after the pumping radiation has terminated. If  $\Delta\nu$  is such that  $t_v$  becomes comparable to the pump pulse duration then the phase grating moves during the time of the pump pulse,  $t_p$ . If  $t_v$  is less than  $t_p$  then the grating moves through several periods,  $\Lambda$ , during  $t_p$ . If  $t_d$  is fast enough ( $t_d < t_v$ ) then the grating moves but remains sharp having good fringe contrast. If  $t_d$  is comparable to or greater than  $t_v$  ( $t_d > t_v$ ) then the grating is partially washed out as it moves leading to loss of contrast and reduced diffraction efficiency. For  $t_d \gg t_v$  the grating is totally washed out and no FRS can be expected.

The value of the diffusion time therefore places a limit on the spectral purity and the alignment tolerances in an FRS experiment. First, two beam interference from a single laser usually involves a beam splitter and two different paths to a region of beam crossing where the interference takes place. If the path length difference exceeds the temporal coherence length of the radiation, then random phase differences cause the interference pattern to move rapidly back and forth in a direction perpendicular to the fringe planes. If the path length difference is much less than the coherence length, then the fringe pattern will be fixed in space. Even though the instantaneous frequency of the radiation changes in a random way throughout the spectral interval  $\Delta\nu$ , the frequencies of the two beams are precisely matched for matched pathlengths. If the path difference is less than the coherence length but still represents a significant part of that coherence length then we must be concerned with the frequency mismatch of the two beams and any washout of the fringes due to the finite thermal diffusion time. As discussed above, we require that the diffusion time be rapid enough that the phase grating follows the moving interference pattern. We require

that  $t_v > t_d$  or  $\Delta\nu < (t_d)^{-1}$ ; that is, the difference frequency must be on the order of or less than the reciprocal of the diffusion time. At small angles,  $t_d$  is on the order of  $\mu\text{sec}$ , whereas for a maximum angle of  $2\theta = \pi$  (backscattering)  $t_d$  is on the order of  $\text{nsec}$ . Tolerable values of  $\Delta\nu$  may therefore range from MHz to GHz.

Left Blank Intentionally  
(page 24)

6  
NITROGEN LASER PUMPED DYE LASER

The radiation source used for the initial experiments in this program was a Molectron SP-10 nitrogen laser pumped dye laser. The manufacturer specified spectral linewidth was 0.3 nm FWHM or  $12 \text{ cm}^{-1}$  (360 GHz) corresponding to a coherence length of 0.8 mm. With a cavity length of 12 cm and intermode spacing of 1.25 GHz, this represents about 300 longitudinal modes. Recognizing a need for greater spectral purity, fewer longitudinal modes, and a longer coherence length, a Laser Sciences, Inc. grazing incidence grating dye laser was purchased and is shown in Figure 6.1. The nitrogen laser from the Molectron SP-10 was used as the pump source, and the LSI laser possessed the characteristics presented in Table II. Although the manufacturer specified the linewidth to be 0.01 nm or  $0.4 \text{ cm}^{-1}$  (12 GHz) implying a 25 mm coherence length, we measured the coherence length to be only 3 mm implying the linewidth to be 0.08 nm or  $3.3 \text{ cm}^{-1}$  (100 GHz). Since the laser cavity length is 7.5 cm and intermode spacing is 2 GHz, we expect to have 50 longitudinal modes oscillating.

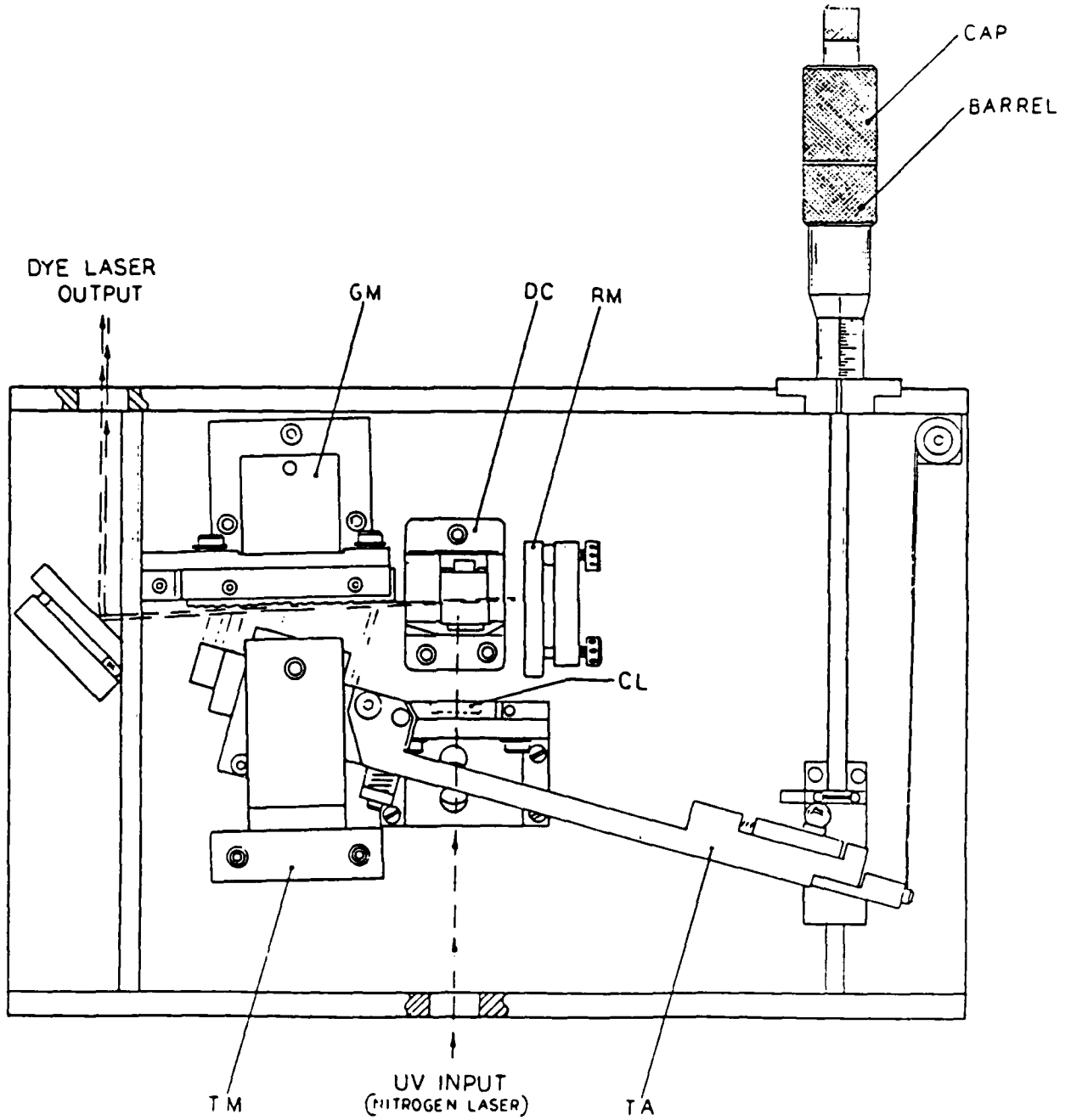


Figure 6.1 LSI Grazing Incidence Dye Laser.  
 GM - Grating Mount; DC - Dye Cell; RM - Rear Mirror; TM - Tuning Mirror  
 Mount; TA - Tuning Arm; CL - Cylindrical Lens.

TABLE II  
LSI GRAZING INCIDENCE DYE LASER PARAMETERS  
MODEL 337130

(Pump Laser: Molectron SP-10 N<sub>2</sub> laser, 337.1 nm, 10 nsec, 0.2 mJ,  
1.5 x 25 mm)

Pulse length	3 nsec
Pulse energy	26 $\mu$ J at 500 nm and 20 pps
Peak power	10 Kw
Spectral linewidth*	0.08 nm, FWHM 3.3 cm <sup>-1</sup> (100 GHz)
Coherence length*	3 mm
Cavity length	75 mm
Temporal mode spacing	2 GHz
Beam quality	5 mrad 1.3 x (diffraction limit)
Active lasing region	10 mm x 0.1 mm
Polarization	horizontal

\*Measured values; LSI specifies 0.01 nm, 0.4 cm<sup>-1</sup>, 12 GHz, and  
25 mm, respectively.

Left Blank Intentionally  
(page 28)

## SUMMARY AND CONCLUSION

This report presents an analysis of the radiation-matter interaction describing the generation of optically-induced thermal phase gratings and its relation to optical control. The interference of two mutually coherent beams of laser radiation leads to a spatial interference fringe pattern which is converted through thermal absorption into a refractive index phase grating. The real-time phase grating is treated as a thick reflection hologram capable of diffraction or deflecting another beam of laser radiation thereby achieving light control by light. The analysis shows that for our experimental conditions a refractive index change of only  $10^{-3}$  should lead to a phase grating possessing a diffraction efficiency in excess of 20 percent. This corresponds to a thermal grating having a maximum temperature difference of about  $1^{\circ}\text{C}$ . Nanosecond laser pulses having an energy on the order of a microjoule should be able to generate such gratings and will be used in experiments during the third reporting period of this program.

Left Blank Intentionally  
(page 30)

APPENDIX A  
THE THERMO-OPTIC COEFFICIENT FOR FLUIDS

Gases

The refractive index of a material medium is related to the amount of matter affecting the beam propagation. The refractive index of a vacuum is of course 1.0. For a gas, the increase in refractive index as matter is added to the vacuum can be described with good accuracy through the Dale-Gladstone relation [8]

$$(n - 1) = K\rho \quad (\text{A.1})$$

where  $\rho$  is the gas density and the proportionality constant  $K$  depends upon the polarizability or susceptibility of the molecules of gas. The density can be modeled to first order using the ideal gas law resulting in an expression for the thermo-optic coefficient  $dn/dT$ . We can write

$$\left(\frac{dn}{dT}\right)_p = \left(\frac{dn}{d\rho}\right)_p \left(\frac{d\rho}{dT}\right)_p \quad (\text{A.2})$$

where the subscript  $p$  denotes constant pressure. Since volume and density are inversely related parameters ( $\rho = m/V$ ), such that

$$\frac{1}{V} \frac{dV}{dT} = - \frac{1}{\rho} \frac{d\rho}{dT}, \quad (\text{A.3})$$

then, for an ideal gas

$$\frac{1}{V} \left(\frac{dV}{dT}\right)_p = \frac{1}{T}$$

becomes

$$\frac{1}{\rho} \left(\frac{d\rho}{dT}\right)_p = - \frac{1}{T}$$

Differentiating Eq. (A.1) and substituting along with Eq. (A.3) into Eq. (A.2), we have

$$\left(\frac{dn}{dT}\right)_p = \left(\frac{n-1}{\rho}\right)\left(-\frac{\rho}{T}\right) = -\left(\frac{n-1}{T}\right)$$

The thermo-optic coefficient for an ideal gas is therefore inversely proportional to temperature.

### Liquids

For high density gases and liquids, the refractive index and density are related by the Lorentz-Lorentz law [8, 9] (cf. the Clausius-Mossotti law [10])

$$\left(\frac{n^2 - 1}{n^2 + 2}\right) = K' \rho \quad (\text{A.4})$$

where again the proportionality constant, here  $K'$ , is determined by the nature of the material medium. Differentiating, we have

$$\begin{aligned} \frac{d\rho}{dn} &= \frac{1}{K'} \left[ \frac{2n}{n^2 + 2} - \frac{(n^2 - 1)2n}{(n^2 + 2)^2} \right] \\ &= \frac{1}{K'} \frac{6n}{(n^2 + 2)^2} \end{aligned}$$

Using (A.4) we can eliminate the  $K'$  to obtain

$$\frac{dn}{d\rho} = \frac{(n^2 - 1)(n^2 + 2)}{6n\rho} \quad (\text{A.5})$$

Substituting Eq. (A.5) into Eq. (A.2) and using Eq. (A.3), we have for the thermo-optic coefficient for fluids

$$\frac{dn}{dT} = -\frac{(n^2 - 1)(n^2 + 2)}{6n} \beta_V \quad (\text{A.6})$$

where  $\beta_V$  is the volume coefficient of thermal expansion

$$\beta_V = \frac{1}{V} \frac{dV}{dT} = -\frac{1}{\rho} \frac{d\rho}{dT}$$

Using tabulated values of  $\beta_V$  [11], the computed values of  $dn/dT$  are in good agreement with measured values of  $dn/dT$  [12]. This is

particularly valuable since  $\beta_v$  is readily available for many liquids but  $dn/dT$  is more difficult to find.

We note in closing that although the relation in Eq. (A.6) is quite accurate for liquids, it remains to be determined how accurate it is for plastics, glasses or crystals.

Left Blank Intentionally

(page 34)

APPENDIX B  
REFRACTIVE INDEX EFFECTS UPON A FOCUSED GAUSSIAN BEAM

Snell's law leads to refraction at an interface. The focal length,  $f$ , of a lens is therefore extended due to the refractive index of the medium as shown in Figure B.1. That is,

$$f' = f + L \left( \frac{\tan \theta}{\tan \theta'} - 1 \right)$$

or,

$$f' \approx f + L(n - 1)$$

for small  $\theta$  or large  $f$ /number. What impact does refractive index have upon (a) the focal spot diameter,  $\delta$ , (b) the length of the focal region,  $l$ , and (c) the fringe spacing of the interfering beams,  $\lambda$ ?

- (a)  $\delta' = \delta$  The sine of the angle of divergence for a diffraction limited spot,  $\delta$ , is proportional to the ratio of the optical wavelength in the medium to the diameter of that spot. In air we have

$$\sin 2\theta = n \frac{\lambda_0}{\delta}$$

and in the medium

$$\sin 2\theta' = n \frac{\lambda}{\delta}$$

where  $n$  is a proportionality constant ( $n = 4/\pi$  for Gaussian beams). By Snell's law  $\sin \theta = n \sin \theta'$  and we know that  $\lambda = \lambda_0/n$ . These equations lead to  $\delta' = \delta$  in the small angle approximation.

- (b)  $l' = n l$  The length of the focal region is defined through

$$\tan \theta = \frac{\delta/2}{l/2}$$

or

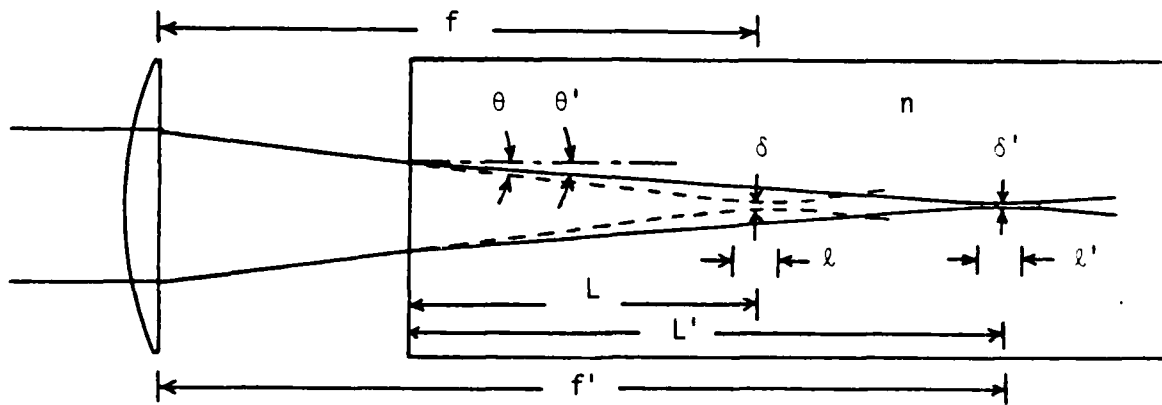


Figure B.1 Change of focus in a medium of refractive index  $n$

$$\tan \theta' = \frac{\delta'/2}{\ell'/2} .$$

Using Snell's Law and  $\delta' = \delta$ , we have

$$\ell' = n\ell .$$

(c)  $\Lambda' = \Lambda$  Two beams of radiation which cross at an angle  $\phi$  in free space produce fringes of spacing  $\Lambda$  such that

$$\lambda_0 = 2\Lambda \sin \phi/2 .$$

If they are allowed to cross in a medium, we have

$$\lambda = 2\Lambda' \sin \phi'/2 .$$

Using Snell's Law and  $\lambda = \lambda_0/n$ , we see that the fringe spacings are the same

$$\Lambda' = \Lambda .$$

Left Blank Intentionally  
(page 38)

APPENDIX C  
OPTIMIZING THE ABSORPTION COEFFICIENT

In the Appendix of the semi-annual report for this program [1], we discussed the optimization of the absorption coefficient to maximize the gain for an injected signal in stimulated thermal Rayleigh scattering (STRS). We saw that the best choice of  $\alpha$ , the absorption coefficient, is predicted to be equal to the reciprocal of the length of the sample in the direction of propagation. In this section we wish to make similar arguments to show that for STRS in generator experiments or forced Rayleigh scattering, the best choice of  $\alpha$  has a value equal to the reciprocal of the length from the entrance window of the sample to the focal region of focused radiation.

Equation (4.5) shows that the refractive index change,  $\Delta n$ , in the focal volume located a distance  $z_f$  from the entrance face of the sample depends upon  $\alpha$  in a non-monotonic way. Qualitatively, a large value of  $\alpha$  is desired for efficient conversion of laser radiation to thermal energy but too high a value of  $\alpha$  leads to attenuation of the laser energy before it can work effectively in the focal volume. This is shown quantitatively by rewriting Eq. (4.5) keeping only the functional dependence upon  $\alpha$

$$\Delta n(r) = \kappa(r) \alpha e^{-\alpha z_f}$$

where  $\kappa(r)$  is a proportionality factor. To find the best choice for  $\alpha$  where  $\Delta n$  is a peak value, we differentiate and equate to zero

$$\frac{d(\Delta n)}{d\alpha} = \kappa(r) e^{-\hat{\alpha} z_f} + \kappa(r) \alpha e^{-\hat{\alpha} z_f} (-z_f) = 0$$

or

$$1 - \hat{\alpha} z_f = 0.$$

We see that  $\hat{\alpha}$ , the optimum choice for  $\alpha$ , is equal to the reciprocal of the distance to the focus

$$\hat{\alpha} = \frac{1}{z_f} .$$

Left Blank Intentionally  
(page 40)

APPENDIX D  
THERMAL DIFFUSION

Transient heat conduction or thermal diffusion is described by  
[13]

$$\frac{dT}{dt} = D\nabla^2 T \quad (D.1)$$

where  $T$  is the deviation of the temperature from its equilibrium value. The thermal diffusivity of the material medium is

$$D = \frac{\lambda_T}{\rho c_p} \quad (D.2)$$

where  $\lambda_T$  is the thermal conductivity,  $\rho$  is the mass density and  $c_p$  is the specific heat at constant pressure. For our particular situation of a thermal phase grating,  $T$  is a sinusoidal function which can be expressed as

$$T(x, t) = \Delta T(t) \cos Kx \quad (D.3)$$

where  $\Delta T$  is the temperature half-amplitude and  $K$  is a spatial frequency

$$K = \frac{2\pi}{\Lambda},$$

$\Lambda$  being the spatial wavelength of the sinusoid. Applying the  $\nabla^2$  operator we have

$$\begin{aligned} \nabla^2 T &= -K^2 \Delta T \cos Kx \\ &= -K^2 T \end{aligned}$$

Equation (D.1) may therefore be rewritten as

$$\frac{dT}{dt} = -DK^2 T .$$

Integrating, we obtain

$$\int_{T_0}^T \frac{dT'}{T'} = -DK^2 \int_0^t dt'$$

$$\ln T - \ln T_0 = -DK^2 t$$

$$\ln \frac{\Delta T}{(\Delta T)_0} = -DK^2 t$$

$$\Delta T = (\Delta T)_0 e^{-DK^2 t}$$

using Eq. (D.3). The amplitude of the stationary thermal wave can be seen to decay exponentially with a time constant of

$$t_d = \frac{1}{DK^2} . \quad (D.4)$$

We may use Table I in conjunction with Eqs. (D.2) and (D.4) to calculate the thermal decay time. Using the physical parameters provided in Table I, the thermal diffusivity for liquid media is calculated to be on the order of  $10^{-3} \text{ cm}^2 \text{ sec}^{-1}$ . For counter-propagating beams where  $2\theta = 180^\circ$  (see Figure 2.1),  $\Lambda$  is a minimum (and so is  $t_d$ ), equal to  $\lambda/2$ . The thermal decay time in a liquid for such a grating is approximately 2.5 nsec and is typical for STRS. For small angle ( $\sim 0.1$  rad) diffraction where  $\Lambda$  is about  $10\lambda$ , decay times are approximately 5  $\mu\text{sec}$  and correspond to thermal diffusion in forced Rayleigh scattering (FRS) as shown in Table III.

It is interesting to note that the reciprocal of the lifetime of the thermal grating is equal to the linewidth for Rayleigh scattering i.e.,

$$\Gamma_R = \frac{1}{2t_d} = \frac{DK^2}{2} .$$

Table III  
CHARACTERISTICS FOR STRS AND FRS

<u>Scattering</u>	<u><math>2\theta</math></u>	<u><math>\Lambda</math></u>	<u><math>t_d</math></u>
STRS	$\pi$	$\lambda/2$	25 nsec
FRS	0.1	$10\lambda$	4 $\mu$ sec

Left Blank Intentionally  
(page 44)

APPENDIX E  
REFLECTION HOLOGRAM DIFFRACTION EFFICIENCY

Forced Rayleigh scattering entails the interference of two pump beams in an absorbing medium to generate a thermal phase grating which is able to diffract radiation from a third beam as shown in Figure 4.1. The two beam interference essentially "writes" a hologram which is "read" in real time by the third beam. The geometry of interaction is similar to that of a reflection hologram and as such can be analyzed using the equations of holography [14]. The diffraction efficiency for a phase reflection hologram is

$$\eta = \frac{I_d}{I} = \left\{ \frac{\xi_r}{\zeta_r}^2 + \left[ 1 - \left( \frac{\xi_r}{\zeta_r} \right)^2 \right] \left[ \coth(\zeta_r^2 - \xi_r^2)^{1/2} \right]^2 \right\}^{-1}$$

$$\xi_r = \Delta\phi \frac{2\pi n_0}{\lambda_r} \delta \cos \phi \quad (E.1)$$

and

$$\zeta_r = \frac{\pi \Delta n \delta}{\lambda_r \sin \phi} ,$$

where  $I$  and  $I_d$  are the incident and diffracted radiation intensities,  $\phi$  is the angle which the reading radiation propagation vector makes with respect to the grating fringe planes,  $\Delta\phi$  is the mismatch between  $\phi$  and the Bragg angle ( $\Delta\phi = \phi - \phi_b$ ),  $n_0$  is the refractive index of the medium,  $\Delta n$  is the peak-to-valley change in refractive index due to the sinusoidal phase grating, and  $\delta$  is the width of the hologram, here equal to the focused waist diameter. If we assume that the Bragg condition is satisfied, we have  $\xi_r = 0$ , and Eq. (E.1) simplifies to

$$\eta = (\tanh \zeta_r)^2 .$$

For small values of  $\zeta_r$  (i.e.,  $\eta \ll 1$ ),  $\eta$  can be approximated as

$$\eta \approx \zeta_r^2$$

and  $\eta$  is therefore proportional to  $(\Delta n)^2$ .

If  $\phi$  is well matched to the Bragg angle  $\phi_b$  such that  $\Delta\phi = \xi_r = 0$ , then Eq. (E.1) simplifies to

$$\eta = \tanh^2 \zeta_r = \left[ \frac{e^{\zeta_r} - e^{-\zeta_r}}{e^{\zeta_r} + e^{-\zeta_r}} \right]^2$$

and is plotted in Figure E.1 for conditions typical of our experiments:

$$\lambda_r = 0.5 \text{ } \mu\text{m}$$

$$\delta = 10 \text{ } \mu\text{m}$$

$$\phi = 0.1 \text{ rad}$$

$$n_0 = 1.5$$

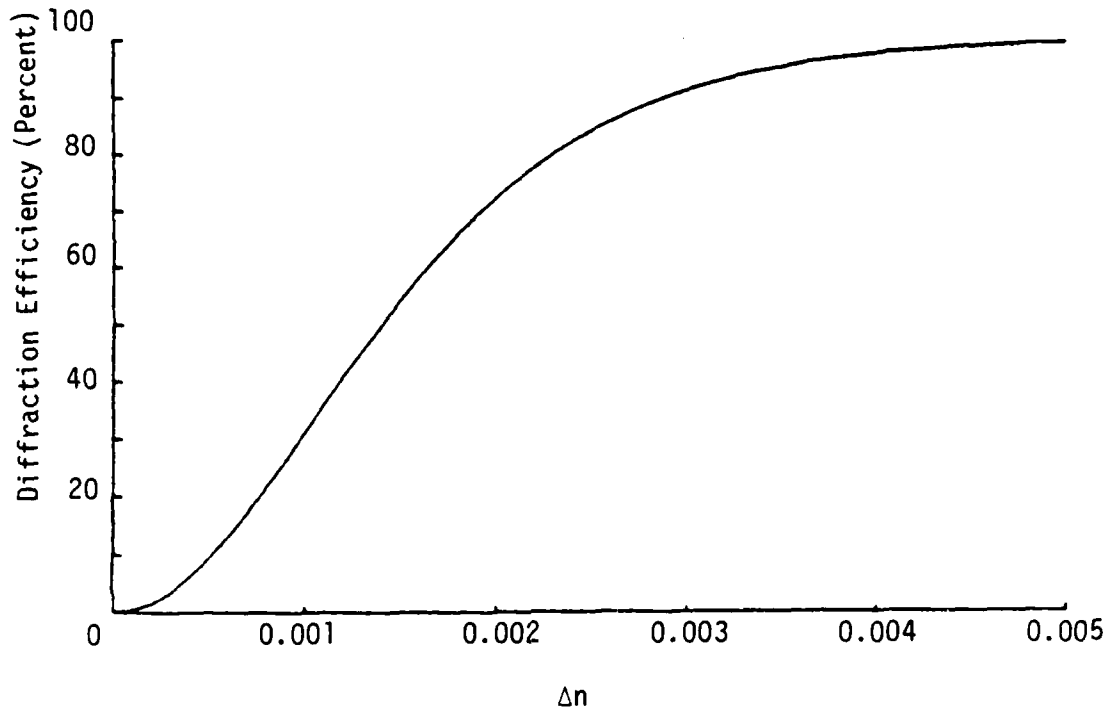


Figure E.1 Diffraction efficiency for a thick reflective phase hologram as a function of refractive index amplitude.

Left Blank Intentionally  
(page 48)

Appendix F

Optical Switching Using Stimulated  
Rayleigh Scattering

Lauren M. Peterson

Proceedings of the SPIE, Vol. 625  
Optical Computing, p. 87-93,  
Los Angeles, January 1986.

# Optical Switching Using Stimulated Rayleigh Scattering

Lauren M. Peterson

Infrared and Optics Division, Environmental Research Institute of Michigan  
P.O. Box 8618, Ann Arbor, Michigan 48107

## Abstract

The use of stimulated light scattering as a means for achieving optical control functions directed toward an optical computer is described. Stimulated thermal Rayleigh scattering is seen to be a preferred nonlinear optical mechanism when compared with the more familiar stimulated Raman and stimulated Brillouin scattering. It possesses the highest gain, the lowest threshold, and scattered radiation which is approximately the same frequency as the inducing radiation. Optical control functions such as optical bistable switching, optical amplification and optical limiting or clipping are described.

## Introduction

Optical radiation passing through a material medium is weakly scattered in all directions by random fluctuations in the index of refraction. This scattering process may be viewed as a diffraction phenomenon where the random index fluctuations are Fourier decomposed into a three-dimensional collection of sinusoidal phase gratings representing a continuum of spatial frequencies and a continuum of orientations in space, i.e., a continuum of grating k-vectors. Random acoustic disturbances in the medium lead to phase gratings which propagate at the speed of sound, and random temperature variations in the medium lead to non-propagating phase gratings with finite lifetimes. The former leads to spontaneous Brillouin scattering and the latter leads to spontaneous Rayleigh scattering.

Experiments using high power ruby lasers<sup>1-4</sup> showed that those Fourier components which led to backscattered radiation would beat with the forward traveling laser radiation in the presence of a nonlinear medium to generate a density wave which precisely matches the phase grating which causes the spontaneous scattering. The magnitude of the phase grating is thereby amplified which leads to more backscattering and so on. This process continues on a subnanosecond time scale and, if the power density of the laser is adequate and the material medium is sufficiently nonlinear, then most of the laser radiation can be redirected into the backward direction. Such intense scattering is referred to as stimulated scattering. If the amplified material wave is a propagating acoustic wave (acoustic phonon) and the radiation is Doppler shifted, this is stimulated Brillouin scattering (SBS). If the material wave is a nonpropagating thermal wave, this is stimulated thermal Rayleigh scattering (STRS). (Stimulated Raman Scattering, SRS, and Stimulated Rayleigh Wing Scattering, SRWS, are analogous processes involving optical phonons and orientational fluctuations, respectively).

## Theory for Absorption-Assisted STRS

The theory for absorption-assisted STRS has been thoroughly developed by Herman and Gray<sup>5,6</sup>; and found to favorably agree with experimental observations<sup>3</sup>. The theoretical development of Herman and Gray deals with the electromagnetic wave using Maxwell's wave equation and treats the thermal and density fluctuations of the material medium using the linearized hydrodynamic equations. The fluctuations in the medium are coupled to the electromagnetic wave through the time dependent nonlinear polarization,

$$P_{NL}(t) = \frac{\rho(t)\alpha_{mol}}{M} \left(\frac{n+2}{3}\right)^2 E(t) \quad (1)$$

where  $\rho(t)$ : mass density of medium ( $\text{gm cm}^{-3}$ )  
 $\alpha_{mol}$ : molecular polarizability ( $\text{cm}^3$ )

$\left(\frac{n+2}{3}\right)^2$ : local field correction

$E(t)$ : laser radiation field amplitude ( $\text{statv cm}^{-1}$ )  
 $M$ : molecular mass ( $\text{gm}$ )

A field dependent  $\alpha_{mol}$  leads to stimulated Raman scattering. A field dependent  $\rho$  leads to stimulated Brillouin scattering if  $\rho$  is driven by electrostriction, and to STRS if  $\rho$  is driven by thermal absorption.

Growth of the scattered radiation field,  $E_S$ , and depletion of the pumping laser field,  $E_L$ , can be described using the coupled equations

$$\frac{\partial E_L}{\partial z} = -\frac{\omega_L}{2cn} \chi''(\omega_S) |E_S|^2 E_L - \frac{1}{2} \alpha E_L \quad (2)$$

$$\frac{\partial E_S}{\partial z} = \frac{\omega_S}{2cn} \chi''(\omega_S) |E_L|^2 E_S + \frac{1}{2} \alpha E_S \quad (3)$$

where  $\omega_L$  and  $\omega_S$  are the optical radian frequencies of the laser and scattered radiation, respectively, and  $\chi''$  is the imaginary part of the 3rd order nonlinear susceptibility. The last equation is easily solved if we assume that  $|E_L|^2$  is approximately a constant i.e., if the laser intensity is not depleted. This is a reasonable assumption if the STRS radiation is less than a few percent of the incident laser radiation, but breaks down as the STRS approaches the intensity of the laser radiation itself. Integrating the last equation over the interaction region  $l$ , we obtain

$$E_S(l) = E_S(0) e^{\frac{1}{2}(g-\alpha)l} \quad (4)$$

$$I_S(l) = I_S(0) e^{(g-\alpha)l} \quad (5)$$

where

$$g(\omega_S) = \frac{\omega_S}{nc} \chi''(\omega_S) |E_L|^2 \quad (6)$$

For STRS,

$$\chi''(\omega_S) = (n^2 - 1) \left( \frac{n^2 + 2}{3} \right) \frac{\beta n c \alpha}{\rho_0 c_p} \left[ \frac{(\omega_L - \omega_S)}{(\omega_L - \omega_S)^2 + \frac{1}{4}(\Gamma_L + \Gamma_R)^2} \right] \quad (7)$$

where  $\beta$ : thermal expansion coefficient ( $^{\circ}K^{-1}$ )  
 $\alpha$ : light absorption coefficient ( $cm^{-1}$ )  
 $\rho_0$ : average mass density ( $gm\ cm^{-3}$ )  
 $c_p$ : specific heat at constant pressure ( $erg\ gm^{-1}\ ^{\circ}K^{-1}$ )  
 $\Gamma_L$ : laser spectral full-width at half-height ( $rad\ sec^{-1}$ )  
 $\Gamma_R$ : Rayleigh spectral full-width at half height ( $rad\ sec^{-1}$ )

The spontaneous Rayleigh line width,  $\Gamma_R$ , is the reciprocal of the thermal diffusion time or Rayleigh lifetime,  $\tau_R$ , and can be written as

$$\Gamma_R = \frac{2\Lambda K^2}{\rho_0 c_p} = \frac{2}{\tau_R} \quad (8)$$

where  $\Lambda$ : thermal conductivity ( $erg\ cm^{-1}\ sec^{-1}\ ^{\circ}K^{-1}$ )  
 $D = \Lambda/\rho c_p$ : thermal diffusivity ( $cm^2\ sec^{-1}$ )  
 $K = |k_L - k_S|$ : thermal grating wavevector ( $cm^{-1}$ )

#### Frequency Dependence

The frequency dependence of STRS gain is described by the factor in brackets in Eq. (7) and in Figure 1. Differentiation of the gain with respect to  $\omega_S$  shows that the gain is predicted to be a maximum at  $\omega_S = \omega_L + (\Gamma_L + \Gamma_R)/2$ , an anti-Stokes frequency shift. Since  $\Gamma_R$  is on the order of  $10^{-8}$  sec for typical liquids,  $\Gamma_L$  usually dominates over  $\Gamma_R$  and the predicted frequency off-set of the scattered radiation is essentially equal to one-half of the laser linewidth. In contrast to the other stimulated scattering processes which possess significant Stokes frequency off-sets, the frequency of the STRS is nearly identical to the incident laser radiation. This feature makes STRS valuable for optical computing applications where cascading of control functions is necessary.

Combining Eqs. (6) and (7), the maximum gain for STRS is

$$\hat{g} = \frac{\omega_S}{nc} (n^2 - 1) \left( \frac{n^2 + 2}{3} \right) \frac{\beta n c \alpha}{\rho_0 c_p} |E_L|^2 \left[ \frac{1}{\Gamma_L + \Gamma_R} \right] \quad (9)$$

### Optimum Absorption

Using Eq. (9), maximum gain can be obtained by selecting a material medium possessing the best combination of physical properties. The two parameters at the experimentalists disposal are the absorption coefficient  $\alpha$ , and the laser field amplitude,  $E_L$ . High laser field intensities are obtained by focusing the laser radiation, and different values of  $\alpha$  can be obtained by adding a dye to the material medium.

Since gain is linearly proportional to  $\alpha$ , a heavily absorbing medium is desired provided that the absorption of the laser and scattered radiation is not excessive. Substituting Eq. (9) into Eq. (5), being sure to include the absorption of  $|E_L|^2$ , one can differentiate Eq. (5) using  $\alpha$  as the dependent variable to show that  $I_S$  achieves its maximum when

$$\alpha = \frac{1}{L[1 + (\hat{g}L)^{-1}]^{-1}} \quad (10)$$

where  $L$  is the propagation distance in the absorbing medium. For STRS originating from spontaneous noise (i.e., spontaneous Rayleigh scattering),  $(\hat{g}L)^{-1}$  is much larger than 1 such that the term in square brackets may be ignored. The largest  $\alpha$  and therefore greatest gain,  $\hat{g}$ , corresponds to the smallest  $L$ , but  $L$  may be no smaller than the interaction length  $l$  (usually the focal region of the focused laser radiation), such that

$$\alpha_{\text{optimum}} \approx 1/l. \quad (11)$$

### Optical Bistable Switching

Figure 2 shows the standard experimental configuration for generating stimulated scattered radiation. Since power densities of  $\text{Mw/cm}^2$  are required to see these nonlinear effects, the laser radiation is focused into the material medium. Figure 3(a) depicts the incident laser pulse intensity,  $I$ , as a function of time (typical times correspond to tens of nsec), and the transmitted and backscattered intensities  $I_T$  and  $I_S$ , respectively. Experiments studying SBS show the existence of a distinct threshold which is characteristic of stimulated scattering, followed by strong backscattered radiation. A steady state condition can be observed shortly after the threshold is exceeded<sup>7,8</sup>. It is expected that STRS exhibits similar temporal characteristics.

Figure 3(b) shows that optical bistability is manifested in the stimulated interaction. As the incident radiation increases no backscattered wave is observed until the threshold is exceeded. Beyond threshold the backscattered intensity increases with that of the incident radiation. Once the maximum  $I$  is reached and  $I$  falls to smaller values,  $I_S$  follows the same path until  $I$  approaches its threshold value,  $I_{th}$ , at which point the downward path differs from the upward path. This region of hysteresis or memory is the bistable region and possesses the potential for use as an optically bistable switch.

### Optical Amplification

Equation (5) and the discussion above show that in generator experiments such as depicted in Figures 2 and 3, spontaneous noise behaves as a weak signal which undergoes orders of magnitude ( $\approx e^{30}$ ) of amplification in generating the strong backscattered stimulated radiation. One would expect, and it has indeed been observed experimentally<sup>4,6,9</sup>, that operation below threshold leads to amplification of counter-propagating signal radiation. The primary requirement upon the injected signal radiation is that it be spectrally narrow and match the frequency of the strong pumping radiation. This is most easily accomplished by deriving both the pump and signal beams from the same laser source.

Amplification should also be possible in an off-axis geometry as described in the following section.

### Off-Axis Geometry

The various stimulated scattering mechanisms compete with each other for the laser energy and the one with the largest gain is the one which is stimulated. Suppression of SBS in order to observe SRS is commonly known. It is also well known that a stimulated scattering mechanism competes with itself based upon frequency considerations. Those frequency components with the largest gain dominate, and lead to gain narrowing in stimulated scattering. It is less well known that a given stimulated scattering mechanism also competes with itself based upon geometrical considerations.

Most stimulated scatterings are observed on-axis because the interaction length,  $l$ , in equation (5) is greatest in the backward (or forward) direction such that the

amplification is strongest on-axis. If a resonant cavity is placed off-axis around the interaction region such that the cavity center-line establishes the direction of maximum gain then the stimulated scattering is observed in the off-axis direction. This has been observed with SBS<sup>10</sup>.

The use of cylindrical, or possibly conical optics might also provide a useful means of achieving off-axis gain and switching. Figure 4(a) depicts the line focus obtained when a beam of laser radiation is focused by a cylindrical lens. Spontaneous scattering occurs in all directions and the highest gain is within the line focus where the intensity is the highest. To exceed threshold for stimulated scattering however, requires that the amplification exceed the loss. The amplification is highest along the direction of the line focus and therefore the threshold is first reached in a direction which is at 90° with respect to the axis of the incident laser beam.

It should be noted that the density wave which is amplified in the interaction of Figure 2 using spherical optics has its iso-density planes perpendicular to the directions of propagation of the optical radiation (i.e., the k-vector of the phase grating is at 0° and the k-vectors of the incident and scattered radiation are at 0° and 180°, respectively). Theory shows<sup>11</sup> that gain for stimulated scattering follows a  $\sin^2 \theta/2$  dependence such that backscattering dominates over forward. The use of cylindrical optics utilizes (and amplifies) density waves whose iso-density planes are at 45° with respect to the laser beam axis (i.e., the grating k-vector is at 45° and the k-vectors of the incident and scattered radiation are at 0° and 90°, respectively). By symmetry neither direction along the line-focus is preferred and bidirectional stimulated scattering is expected. A unidirectional output might be obtained by simply placing a mirror in one of the beams of scattered light in order to fold it back to the interaction region for further amplification. The use of conical optics as shown in Figure 4(b) can also provide unidirectional off-axis output since gain is higher in the back direction than in the forward.

Switching and amplification functions can be implemented in the off-axis direction by proper choice of the magnitude of the incident or pump radiation. The off-axis geometries should exhibit those same characteristics depicted in Figure 2. Consider the following four optical control functions:

- a. Self-Switching - if the pump radiation exceeds threshold then the radiation is coupled efficiently to an off-axis direction.
- b. Control-Switching - if the pump radiation is below threshold but above the steady state value, then signal radiation injected along the region of highest gain switches the pump radiation from its on-axis propagation to off-axis propagation.
- c. Amplification - if the pump radiation is well below threshold then signal radiation injected along the region of gain is amplified by coupling energy from the on-axis pump beam into the off-axis direction of the signal beam.
- d. Optical Transistor - operating in the amplification mode, if the pump radiation is amplitude modulated, since the gain is nonlinear, the stimulated scattered radiation is modulated with a greater amplitude.

#### Optical Limiting/Clipping

The last optical control function which we wish to discuss is that of limiting or clipping. Figure 3 shows this most clearly. Once threshold has been exceeded, excessive radiation is converted into stimulated radiation,  $I_s$ , such that the radiation which remains in the incident beam,  $I_T$ , is of nearly constant intensity.

#### Discussion

For a control technique to be useful for optical computing applications, it must be accessible at modest optical energies. Table I shows that absorption-assisted STRS has the highest gain and therefore is the best candidate for low energy operation.

Table I. Typical Gain Factors,  $g$ , Frequency Differences,  $\Delta\nu$ , and Lifetimes,  $\tau$ , of Stimulated Scattering Phenomena

	$g$ (cm/MW)	$\Delta\nu$ ( $\text{cm}^{-1}$ )	$\tau$ (ns)
SBS	0.05	0.1	0.1 to 1
STRS			
a) transparent media	0.0002	$10^{-3}$	20
b) absorption-assisted	0.2	$10^{-3}$	20
SRWS	0.001	50	0.001
SRS	0.002	1000	0.01.
SCS*	0.001	$10^{-2}$	5

\* Stimulated concentration scattering.

The tabulated gain coefficient is 0.2 cm/Mw, although a gain of 0.8 cm/Mw has been observed experimentally using I<sub>2</sub> dye in CCl<sub>4</sub> liquid. (The measured gain coefficient for CCl<sub>4</sub> is in agreement with theoretical predictions.) Examination of equation (6) shows that since gain is highest for high optical intensity then one might expect lowest thresholds for a tightly focused Gaussian (TEM<sub>00</sub>) laser beam. A more careful examination of the focusing of a Gaussian profile beam shows however that the length of the focus,  $l$ , which represents the interaction length, decreases as the square of the focused beam diameter due to diffraction<sup>11</sup>. It can be easily shown that

$$g I_L l = \frac{2gP_L}{\lambda} \quad (12)$$

where  $P_L$  is the power in a TEM<sub>00</sub> laser beam of wavelength  $\lambda$ . It should be noted that the exponential amplification is independent of the focused beam size and the interaction length.

Using the more conservative value for  $g$  of 0.2 cm/Mw and taking  $\lambda$  to be 0.5  $\mu$ m, significant gains should be realized for laser powers in excess of about 100 watts. Actual switching should require one to two more orders of magnitude of optical power, but since the switching time for STRS is on the order of nanoseconds, the switching energy is seen to be on the order of several microjoules. These power and energy requirements are modest and may be improved upon if more efficient materials and techniques are developed.

The cylindrical geometry offers such an improvement in optical efficiency. Again assuming a TEM<sub>00</sub> laser beam and diffraction-limited optics one can determine that

$$g I_L l = \frac{gP_L l}{\lambda} \left[ \frac{l/\lambda}{(f/D)^2} \right] \quad (13)$$

for a cylindrical lens, where  $f/D$  is the effective  $f$ -number of the cylindrical lens being used. The improvement factor of cylindrical optics compared to spherical optics is the quantity in square brackets. It should be possible to make  $l$ , the interaction length, here the length of the line focus, much greater than  $\lambda$ . If a small enough  $f$ -number can be used without deleterious effects due to diffraction then the requirements on  $P_L$  should be considerably less than those computed above for spherical optics.

Absorption-assisted STRS is most readily attained in liquid solvents to which an absorbing dye has been added. Although inorganic and simple organic liquids (alcohols, acetone, etc.) have been used to attain STRS, it may be possible to tailor more complex organics with desirable thermodynamic parameters such as a high thermal expansion coefficient,  $\beta$ , or a high molecular polarizability,  $\alpha_{mol}$  in order to increase the gain coefficient and therefore further lower the power requirements. Critical point phenomena or critical opalescence conditions may be found which drastically modify the thermodynamics such that STRS is enhanced.

#### Summary and Conclusions

Stimulated light scattering appears to be a viable method for achieving optical control functions for application to optical computing. Of the various stimulated scatterings, the best known of which are stimulated Brillouin and stimulated Raman scattering, stimulated thermal Rayleigh scattering, STRS, is clearly the best choice. It possesses the highest gain coefficient and does not suffer from large frequency shifts in its scattered radiation as do the other stimulated scatterings.

Optical control functions such as bistable switching, optical amplification, and limiting or clipping can be achieved with STRS. These can be achieved with a laser source and spherical or cylindrical focusing optics. Switching times are on the order of nanoseconds and optical power requirements are hundreds of watts or less. The use of cylindrical optics offers the potential for off-axis geometries and lower optical power requirements.

#### Acknowledgements

This research was supported by the Advanced Research Projects Agency of the Department of Defense and was monitored by the Air Force Office of Scientific Research under Contract No. F49620-84-C-0067. Significant portions of this paper appear in Reference 12.

### References

1. R.Y. Chiao, C.H. Townes and B.P. Stoicheff, Phys. Rev. Letters 12, 592 (1964).
2. E. Garmire and C.H. Townes, Appl. Phys. Letters 5, 84 (1964).
3. D.H. Rank, C.W. Cho, N.D. Foltz, and T.A. Wiggins, Phys. Rev. Letters 19 (15), 828 (1967).
4. W. Kaiser and M. Maier in Laser Handbook, F.T. Arecchi and E.O. Schulz-DuBouise, eds., North-Holland Publ. Co., 1972.
5. R.M. Herman and M.A. Gray, Phys. Rev. Letters 19 (15), 824 (1967).
6. I. Batra, R. Enns and D. Pohl, Phys. Stat. Sol. (b) 48, 11 (1971).
7. K. Daree and W. Kaiser, Phys. Rev. Letters 26, 817 (1971).
8. M. Maier, Phys. Rev. 166, 113 (1968).
9. W. Rother, Z. Naturf 25a, 1120 (1970); *ibid.* 1136.
10. H. Takuma and D. Jennings, Appl. Phys. Lett. 5(12), 239(1964).
11. A. Yariv, Quantum Electronics, John Wiley and Sons, New York, Second Edition (1975).
12. L. Peterson, Opt. Eng. 25(1), 103 (1986).

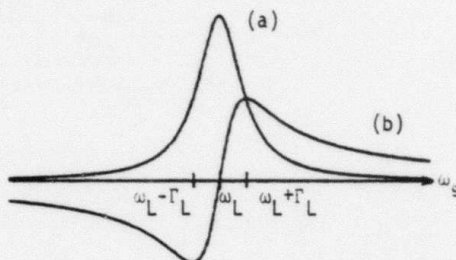


Figure 1. (a) Intensity profile of incident laser radiation. (b) Gain profile for STRS.

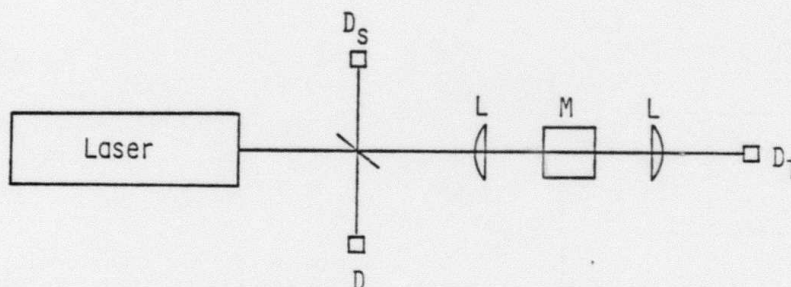


Figure 2. Generator experiment for simulated scattering. Detector D,  $D_T$ , and  $D_S$  measure incident, transmitted and stimulated radiation, respectively, for interactions in nonlinear medium, M.

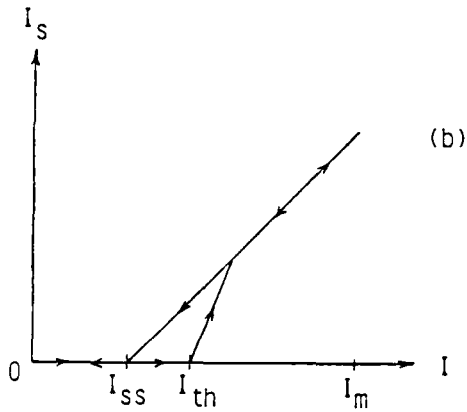
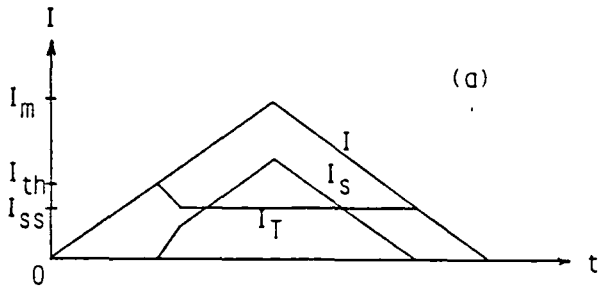


Figure 3. Temporal characteristics of stimulated scattering in (a).  $I$ ,  $I_T$  and  $I_S$  are the incident, transmitted and stimulated radiation respectively. Bistable characteristics of stimulated scattering appears in (b).

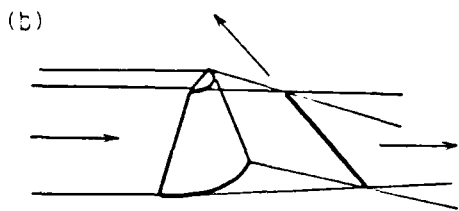
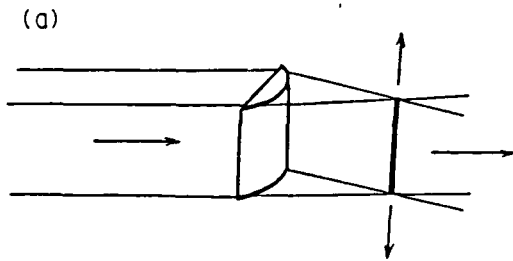


Figure 4. Off-axis geometries for stimulated scattering using cylindrical (a) and conic (b) optics.

## REFERENCES

1. L.M. Peterson, "Optical Switching by Stimulated Thermal Rayleigh Scattering," ERIM Report No. 175900-8-T (DARPA/AFOSR), June 1986.
2. (a) A. Yariv, Quantum Electronics, 2nd edition, John Wiley and Sons, New York (1975) and Optical Electronics, 2nd edition, Holt, Rinehardt and Winston, p. 38 (1976); (b) A. Siegman, "An Introduction to Lasers and Masers," McGraw-Hill Co., p. 313 (1971).
3. K.F. Herzfeld and T.A. Litovitz, Absorption and Dispersion of Ultrasonic Waves, Academic Press, New York (1959).
4. (a) R.M. Herman and M.A. Gray, Phys. Rev. Lett. 19(15), 824, (1967); (b) D.H. Rank, C.W. Cho, N.D. Foltz, and T.A. Wiggins, Phys. Rev. Lett. 19(15), 828 (1967); (c) I. Batra, R. Enns, and D. Phol, Phys. Status Solidi (B) 48, 11 (1971); (d) W. Kaiser and M. Maier, in Laser Handbook, F.T. Arecchi and E.O. Schulz-DuBouise, eds., North-Holland Publ. Co., New York (1972).
5. P.A. Fluery and R.Y. Chiao, J. Acoust. Soc. Amer. 39, 751 (1966).
6. AIP Handbook, D.E. Gray, editor, 2nd edition, McGraw-Hill, Inc. (1963).
7. D.W. Pohl, "Forced Rayleigh Scattering," IBM J. Res. Deve. 23 (5) (1979), 604; see special issue on dynamic gratings and 4-wave mixing, IEEE J. of Quant. Electr. QE-22 (8), pp. 1194-1542 (1986).
8. R.S. Longhurst, Geometrical and Physical Optics, Second Edition, John Wiley and Sons, New York, 1967.
9. J. Reitz and F. Milford, Foundations of Electromagnetic Theory, Addison-Wesley, 1960.
10. J.A. Stratton, Electromagnetic Theory, McGraw-Hill, New York, 1941.
11. AIP Handbook, pp. 4-75.
12. Ibid., pp. 6-90.
13. Ibid., pp. 4-79.
14. R.J. Collier, C.B. Burkhardt, L.H. Lin, Optical Holography, Academic Press, New York, 1971, p. 256.
15. Y.R. Shen The Principles of Nonlinear Optics, Wiley Interscience, 1984.